



ELSEVIER

Physica B 201 (1994) 374–379

PHYSICA B

High magnetic field tunneling transport in a double quantum well–triple barrier resonant tunneling diode

L.D. Macks^a, S.A. Brown^a, R.P. Starrett^a, R.G. Clark^a, M.R. Deshpande^b, M.A. Reed^{b,*},
C.J.L. Fernando^c, W.R. Frensley^c, Richard J. Matyi^d

^aNational Pulsed Magnet Laboratory, School of Physics, University of New South Wales, P.O. Box 1, Kensington, NSW 2033, Australia

^bDepartments of Electrical Engineering and Applied Physics, Yale University, New Haven, CT 06520, USA

^cEric Jonsson School of Engineering & Computer Science, University of Texas at Dallas, Richardson, TX 75083, USA

^dDepartment of Material Science and Engineering, University of Wisconsin-Madison, Madison, WI 53706, USA

Abstract

We have measured the magnetotransport of double GaAs quantum well–triple AlAs barrier resonant tunneling heterostructures in pulsed magnetic fields up to 48 T, and temperatures down to 0.3 K. The tunneling structure is designed for a near-simultaneous (triple) resonance, under bias, of the quantum well energy levels and the lowest quasi-2D emitter state. The fan chart of the $I(V)$ resonances is more complex than that of a single quantum well since both emitter–well and well–well transitions can occur, which can be discriminated by voltage dependence. In addition to transitions corresponding to the emission of an LO phonon, we also observe at high field a transition which may correspond to the absorption of an LO phonon (emitter–well). Shubnikov–de Haas oscillations in the tunnel current of all resonances are observed. At the near-triple resonance, corresponding to a populated 2D well density of $n_S = 4.5 \times 10^{11} \text{ cm}^{-2}$, a SdH peak (at 0.3 K) is observed at 29 T, assigned to a Landau level filling factor of $\frac{3}{2}$. This peak weakens by 2 K, whereas the integer filling factor peaks are unchanged with temperature.

Magnetotransport is a useful tool to investigate scattering mechanisms in electron tunneling structures [1–5]. In resonant tunneling junctions, the application of a magnetic field B perpendicular to the plane of the barriers and well(s) quantizes the already quasi-bound levels into Landau levels of index n , both for elastic [1] and phonon-assisted [2–5] resonant tunneling. In this paper, we report pulsed-magnetic field measurements up to 48 T of a triple-barrier resonant tunneling structure.

The triple-barrier, double-well GaAs/AlAs resonant tunneling structure investigated was grown by MBE. The structure consisted of the following layers grown on a n^+ GaAs (001) substrate; a $0.5 \mu\text{m } n^+$ GaAs

(Si: $\sim 1.5 \times 10^{18} \text{ cm}^{-3}$) buffer and bottom contact, with graded doping at the end (to i -GaAs in 100 \AA); $150 \text{ \AA } i$ -GaAs spacer layer; $40 \text{ \AA } i$ -AlAs barrier; $50 \text{ \AA } i$ -GaAs well; $15 \text{ \AA } i$ -AlAs barrier; $80 \text{ \AA } i$ -GaAs well; $40 \text{ \AA } i$ -AlAs barrier; $150 \text{ \AA } i$ -GaAs spacer layer; and a $0.5 \mu\text{m } n^+$ GaAs (Si: $\sim 1.5 \times 10^{18} \text{ cm}^{-3}$) top contact, with graded doping at the beginning (from i -GaAs in 100 \AA). Mesa diodes (ranging from $64 \mu\text{m}$ to $2 \mu\text{m}$ squares) were fabricated by standard photolithography and wet chemical etching, passivated with silicon nitride and polyimide, and contacted by bonding pads for low temperature measurements.

Fig. 1 (a)–(c) shows calculated conduction band profiles of the structure. The model used to calculate the band profile is a self-consistent Poisson solution, treated in a finite-temperature Thomas–Fermi approximation

* Corresponding author.

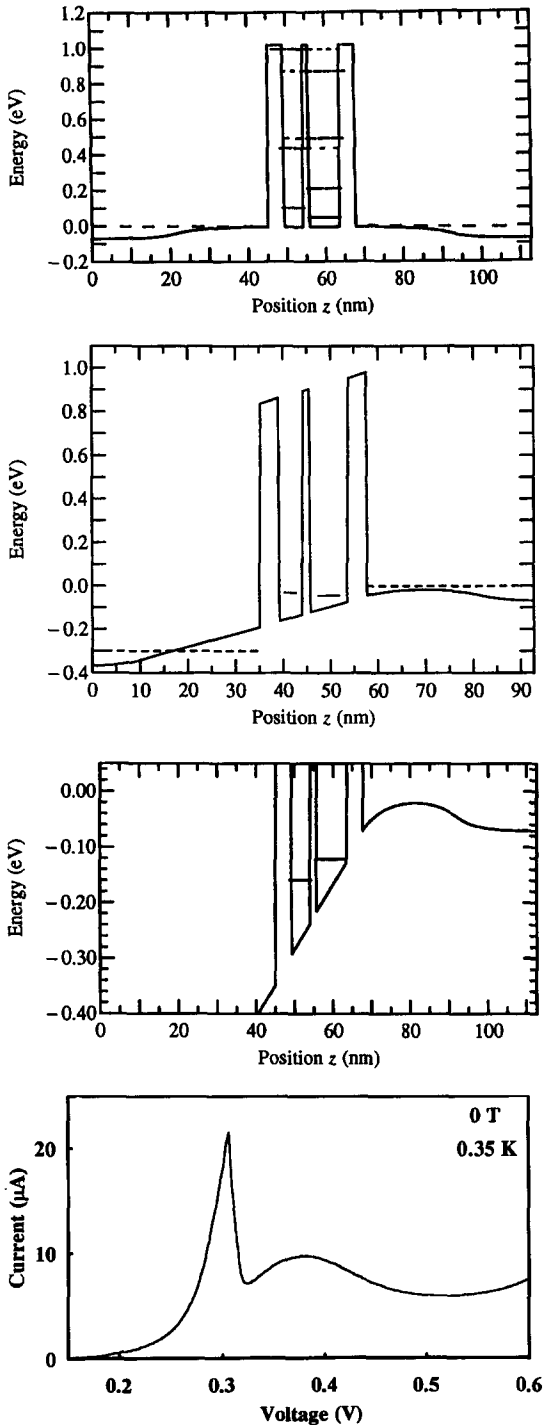


Fig. 1. Calculated band diagrams and $I(V)$ of the 2-well/3-barrier structure. (a) $V=0$. (b) $V=305$ mV. (c) $V=602$ mV (expanded view). (d) $I(V)$ of a $(64 \mu\text{m})^2$ device.

[6]. The model does not include charge in the well; significant charge in the well(s) with respect to the emitter would result in a perturbation of the predicted resonances and a quantitative comparison of experiment with the model is difficult in this regime. The quantum well widths are chosen such that, at “resonant” bias, the lowest quasi-bound well states of the two wells are near a simultaneous line up with the lowest bound state in the emitter accumulation layer (a triple resonance). This situation corresponds to electron injection from the top contact (emitter) into the 80 \AA well first; hereafter, this will be referred to as well #1. Likewise, the further downstream well (50 \AA) is denoted as well #2, and the adjacent (bottom) contact is defined as the collector. Fig. 1(a) shows the quantum well states at no applied bias; the energies (referenced to the Fermi level) are 47 meV for well #1, and 101 meV for well #2. Fig. 1(b) shows the band profile at $V=305 \text{ mV}$, and Fig. 1(c) at 602 mV . Using this model, we can calculate the voltage/energy conversion ratio α for position of the quantum well states; for well #1 $\alpha = 3.56 \text{ mV/meV}$, for well #2 $\alpha = 2.34 \text{ mV/meV}$, and for the difference between the well states $\alpha = 6.74 \text{ mV/meV}$. Over the range 0 – 650 mV , α was observed to be constant, though this would clearly deviate at higher applied bias.

The experimental $I(V)$ at 0.35 K of the $64 \mu\text{m}$ square device presented here, in the region of the triple resonance, has a $B=0$ peak at $V=305 \text{ mV}$, FWHM of 30 mV , and a current density of 0.49 A/cm^2 (Fig. 1(d)). This was compared to a similar heterostructure, sequentially grown and nominally identical except for slightly different quantum well and inter-well tunnel barrier thicknesses (specifically, 65 \AA and 50 \AA wells and a 20 \AA inter-well barrier). The comparison structure exhibited a peak current density of 9.2 A/cm^2 , which argues for a better triple resonance. The lower current density of the structure whose magnetotransport is presented here, as compared to the comparison structure (detailed magnetotransport on the companion structure has not yet been performed), suggests that the present structure may not be exactly simultaneous. Calculations using the as-grown material parameters indicate that the observed resonance is indeed not exactly simultaneous; theoretically $E_{\#1} = E_{\#2}$ at 360 mV , 55 mV higher than the observed resonance, indicating that $E_{\#1}$ has passed through the lowest bound emitter prior to $E_{\#1} = E_{\#2}$.

The sample was mounted in a ^3He cryostat in the bore of a 20 ms , 60 T pulsed magnet coil. The voltage across the sample was ramped near to the peak of the pulsed magnetic field and the current measured simultaneously so that all $I(V)$ measurements were performed with the magnetic field within 2% of its maximum value

(Fig. 2(a)). The total length of the voltage ramp generated is 2 ms ($V = 0$ to V_{\max} and back to $V = 0$). A RuO_2 thermometer was mounted close to the sample and the temperature monitored before and after each magnetic field pulse. Fig. 2(b) shows selected $I(V)$ curves derived from $I(t)$, $V(t)$ data at two magnetic fields. The $I(V)$ measurements using the fast voltage ramp necessary for pulsed field experiments were identical to data obtained using conventional static techniques. Hysteresis was observed at high magnetic field (Fig. 2(b)), which has been observed previously in a double barrier structure [7, 8] and explained by charge accumulation in the well.

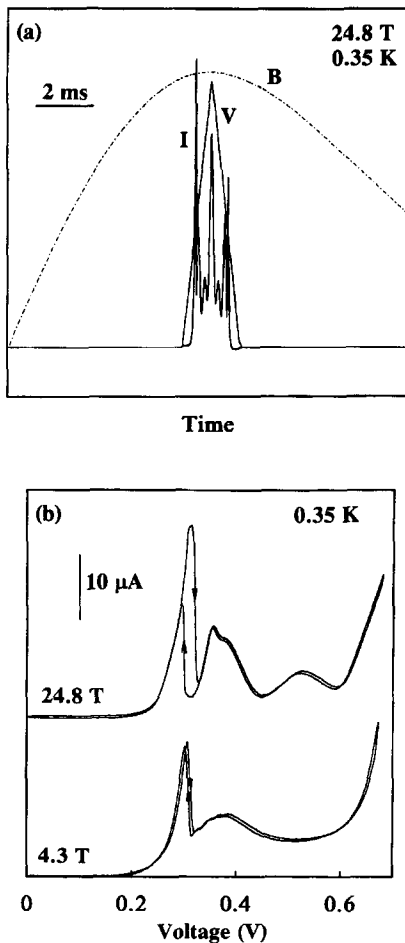


Fig. 2. (a) Current, voltage, and magnetic field versus time for a typical magnetic field pulse ($B_{\max} = 24.8$ T). (b) $I(V)$ curves for 24.8 T and 4.3 T, derived from raw data as in (a), showing hysteresis at high magnetic field.

Fig. 3 illustrates the $I(V)$ in the region of the resonance, as a function of magnetic field parallel to the current flow. A series of resonances beyond the zero-field primary resonance are observed, as well as oscillations in amplitude of the primary resonance with field. All $I(V)$ traces are shown for increasing voltage sweep (from zero).

Fig. 4 illustrates the voltage positions of these resonances as a function of magnetic field. The positions of weak resonances were determined from plots of d^2I/dV^2 versus V (not shown). The fan diagram is significantly more complex in this heterostructure than in a single well resonant tunneling structure [4, 5], due to the possibility of emitter-well and well-well transitions. The primary resonance is evident at 305 mV. The peak position of the primary resonance is observed to oscillate slightly with magnetic field, due to Shubnikov-de Haas oscillations discussed below. The two higher lying resonances that are essentially constant with field also exhibit oscillations. At yet higher applied bias, peaks attributable to inter-Landau level transitions occur.

In a magnetic field applied parallel to the current (perpendicular to the heterointerfaces), the emitter and quantum well energies are quantized into Landau levels with energy $E_n = (n + \frac{1}{2}) \hbar \omega_c$, where $\omega_c = eB/m^*c$ is the cyclotron energy and $n = 0, 1, 2, \dots$ is the Landau level index. The selection rule $\Delta n = 0$ can be broken by interaction with an LO-phonon, causing a series of resonances corresponding to LO-phonon-assisted inter-Landau level tunneling. Additionally, the selection rule can be broken even for the case of no LO-phonon emission, most likely from symmetry-breaking fluctuations in the structure [9].

In a single well structure the main resonant peak, LO-phonon emission resonances (GaAs or AlAs), and the associated inter-Landau level transition fans are easily discernible. However in the present double well structure there now exist three distinct possible processes; (i) emitter to well #1 ($e \rightarrow 1$ "); (ii) well #1 to well #2 ($1 \rightarrow 2$ "); (iii) emitter to well #2 ($e \rightarrow 2$ "). This last process involves a large effective emitter barrier, and measurements in the reverse bias polarity direction indicate a current over three orders of magnitude smaller. For the remaining two possible processes (the "primary" $e \rightarrow 1$, and the inter-well $1 \rightarrow 2$), each may have; (a) a no-LO inter-Landau level fan; (b) a GaAs LO-phonon transition and associated inter-Landau level fan; and (c) an AlAs LO-phonon transition and associated inter-Landau level fan. However, due to the thinness of the AlAs barriers (c) is unlikely [10], and is in fact not observed here.

The most reasonable fit to the inter-Landau level transition fans is given in Fig. 4. Originating from the

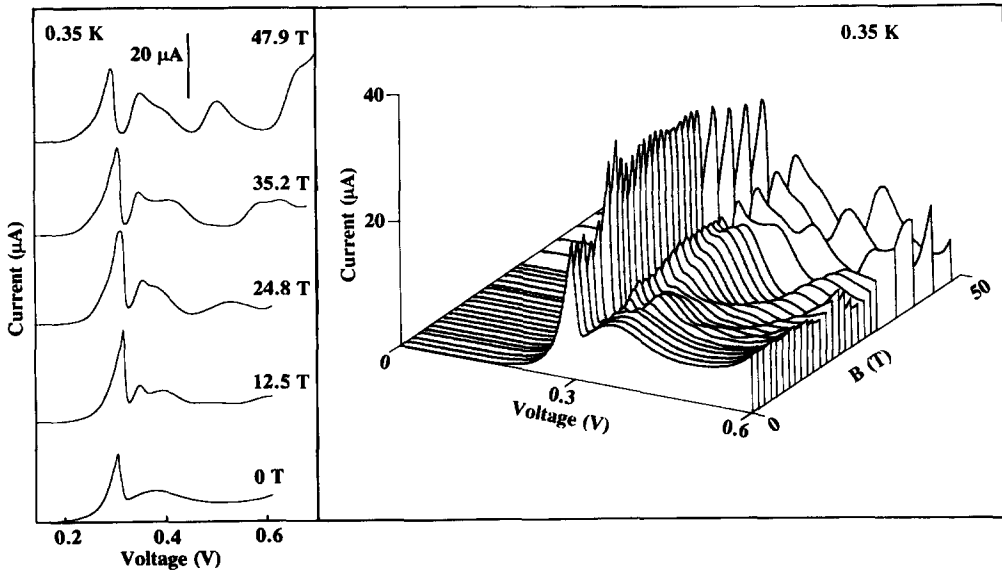


Fig. 3. Pulsed $I(V)$ as a function of B .

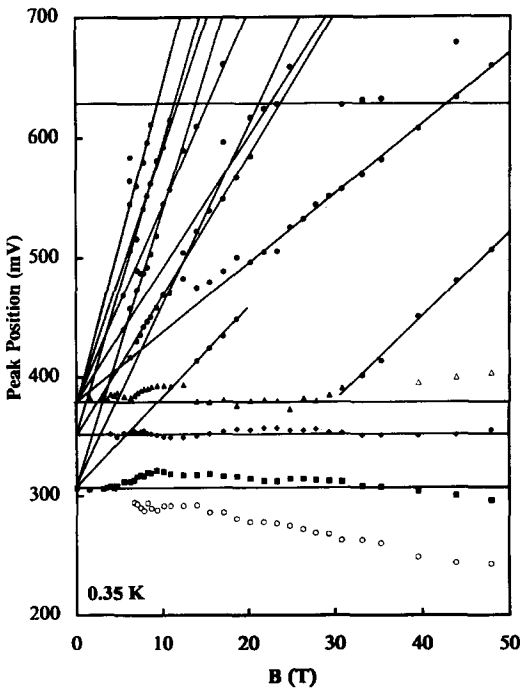


Fig. 4. Peak positions as a function of B . The lines are explained in the text.

$V = 305$ mV primary peak position is a clear $\Delta n = 1$ inter-Landau level transition, in this case with no phonon emission. This is an $e \rightarrow 1$, $\Delta n = 1$ transition. The $\Delta n = 2$ transition is difficult to distinguish due to coincidental overlap with another transition. The $\Delta n = 3$ transition is clearer, due to the difference in slopes from other transitions. The $\Delta n = 1$ transition has a slope of 7.6 mV/T; the calculated slope $\alpha \hbar \omega_C$ is 6.2 mV/T.

At higher bias there exists a fan originating from the $V = 381$ mV ($B = 0$) peak, for $\Delta n = 0$ to $\Delta n = 5$, having a slope ($\Delta n = 1$) of 5.9 mV/T. These transitions are attributable to LO-phonon assisted $e \rightarrow 1$, $\Delta n = 0, \dots, 5$ transitions. The lines for $\Delta n = 2, \dots, 5$ are not fits through data points, but determined from the slope of the $\Delta n = 1$ line. Notice that $\Delta n = 2, 3, 4$ are difficult to unambiguously determine, due to overlap with other transitions; however, when there is no interference, such as the $\Delta n = 5$ line, the fit is excellent. The only major discrepancy for the proposed interpretation is the calculated LO-phonon energy from the $B = 0$ peak positions; using $\alpha = 3.56$ and the measured $V_{no\ LO} - V_{LO}$ of 76 mV gives 21 meV, clearly not in agreement with the expected 36 meV GaAs LO-phonon energy. This discrepancy may be due to the perturbation caused by charge accumulation in the well(s), which will be of significance for the $e \rightarrow 1$ process.

Originating from $V = 350$ mV ($B = 0$, extrapolated), there exists a fan for $\Delta n = 0$ to $\Delta n = 2$, having a slope ($\Delta n = 1$) of 11.3 mV/T. This corresponds remarkably well to both the calculated $1 \rightarrow 2$ crossing (360 mV) and the calculated $\Delta n = 1$ inter-Landau level transition slope ($= 11.7$ mV/T). The assignment to a $1 \rightarrow 2$ transition is supported by data points at higher bias. An LO-phonon-assisted $1 \rightarrow 2$ transition should occur at $\alpha\hbar\omega_{\text{LO}}$, or 602 mV; the line drawn at ~ 630 mV intersects the data points at ~ 32 T, which are sufficiently far away from the $e \rightarrow 1$, $-1\text{LO } \Delta n = 1$ and 2 fans, and the $1 \rightarrow 2$, $\Delta n = 1$ line to be unambiguous. In Fig. 1(c), the calculated energy difference between wells #1 and #2 at 602 mV is 37 meV, in agreement with the GaAs LO-phonon energy. An alternative interpretation of this data is to assign it as an $e \rightarrow 2$ transition; however, the fan slope $\alpha\hbar\omega_{\text{C}}$, current magnitude, and the position of the LO-phonon-assisted transition are in poor agreement with this interpretation.

At $V < V_{\text{primary}}$ there exists very weak structure (open circle data in Fig. 4, observable only in d^2I/dV^2) that appears associated with the primary peak. The slope of the line is $\ll \hbar\omega_{\text{C}}$ even for $\alpha = 1$, indicating that it cannot be $\Delta n = -1$. This is as yet unexplained, but is possibly due to transitions from the $n = 2$ bound emitter state to either of the well states, probably the first [11].

The only other unexplained transitions are for the data points between 30–50 T and 400–500 mV. The assignment of this line to an $e \rightarrow 1$, $\Delta n = 1$ transition gives $\alpha = 3.7$, in good agreement with the calculation. The extrapolated intercept corresponds to an energy of 36 meV lower than the primary peak, in agreement with the GaAs LO-phonon energy, suggesting that this process could be an $e \rightarrow 1$, $\Delta n = 1$ transition with LO-phonon absorption. This process appears unlikely since the number of ambient thermal phonons at 0.35 K is extremely small. Our experience with pulsed field transport measurements in the FQHE regime in single heterojunction and quantum well samples shows that the electron temperature remains at 0.35 K throughout the magnetic field pulse. Additionally, the peak strength at $V > \sim 400$ mV is rather large, whereas it is unobservable at lower voltage (especially for $V < \sim 275$ mV, where it would be unambiguous). Within this interpretation, the phonons would have to be generated by the sample itself, at biases $V > \sim 380$ mV. This implies that the phonons absorbed by electrons undergoing the $e \rightarrow 1$, $+1\text{LO } \Delta n = 1$ process originate from other tunneling electrons that have emitted LO-phonons, especially from the $e \rightarrow 1$, -1LO transitions. To our knowledge, this would be the first observation of a phonon-assisted resonant tunneling transition by phonon self-absorption,

though further systematic studies are needed to exclude more conventional processes.

All of the strong $\Delta n = 0$ peaks exhibit SdH-like oscillations in peak position and current. Fig. 5 illustrates this for the primary ($V = 305$ mV) peak. A striking feature is the appearance of maxima in the peak current at 4.7 T, 9.3 T, 18.7 T and 28.6 T, strongly suggestive of quantum Hall effect (QHE) states associated with a fixed electron density. The density is independently checked against SdH oscillations measured at fixed bias in pulsed magnetic fields as shown in Fig. 6. The inset to Fig. 6 shows the resultant n_s versus V dependence. At low bias, these densities are too small to account for the emitter density. Instead, the SdH oscillations in this bias region must originate from carriers in well #1. The plot of $n_s(V)$ shows an increase from zero at 0.2 V (where conductance is first experimentally observed) and increases with V , as expected. There is an easily discernable change in slope of $n_s(V)$ beyond the primary peak bias. At these higher biases, two effects occur; first, a 2DEG emitter accumulation layer can form; and second, the charge in well #1 is now ejected. Thus, the decrease of dn_s/dV most likely

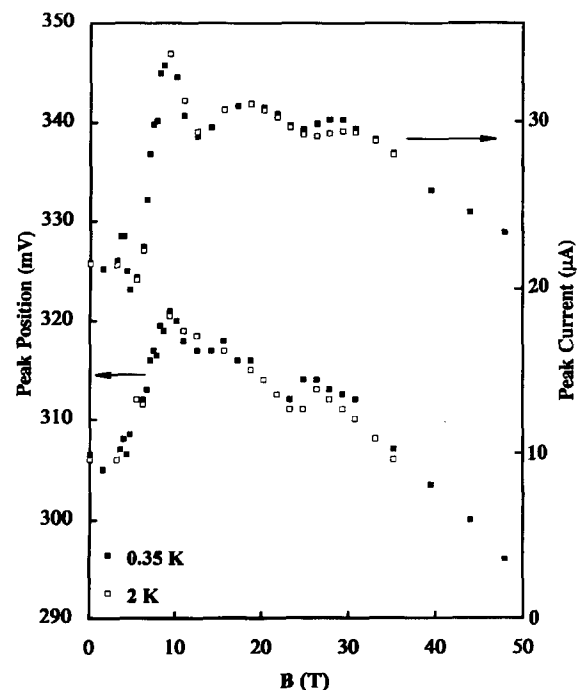


Fig. 5. Primary peak position and current as a function of B , for 0.35 K and 2 K.

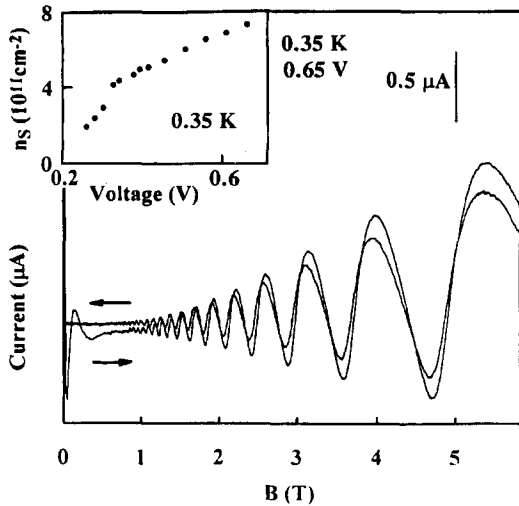


Fig. 6. Current SdH oscillations as a function of B , for $V = 0.65$ V. The inset shows the determined density, as a function of V .

corresponds to a shift of the ‘negative plate’ (and correspondingly the 2DEG responsible for the SdH oscillations) from well #1 to the emitter, resulting in a decreased capacitance of the structure. Estimates from Fig. 6 inset data give fair agreement for the expected dielectric thickness in both cases.

A well #1 density of $n_s = 4.5 \times 10^{11} \text{ cm}^{-2}$ at the primary peak bias is higher than, but in reasonable agreement with the extrapolated density from Fig. 6 and with the following assignment of filling factors for the observed SdH current maxima of the primary peak; at $B = 4.7$ T, $\nu = 4$; at $B = 9.3$ T, $\nu = 2$; at $B = 18.7$ T, $\nu = 1$; and at $B = 28.6$ T, $\nu = \frac{2}{3}$. We tentatively suggest that the observed $\nu = \frac{2}{3}$ peak in our data is indeed a fractional QHE state in well #1. For independent evidence,

we note that at elevated temperature (Fig. 5, $T \rightarrow 2$ K) the $\nu = \frac{2}{3}$ current peak decreases in magnitude whereas the higher filling factor peaks are unchanged. A $\nu = \frac{1}{3}$ fractional QHE state in the 2DEG at the emitter of a single well-double barrier structure has been recently reported in measurements of resonant tunneling carried out in pulsed magnetic fields [12].

In summary, we have measured magnetotunneling in a 2-well/3-barrier structure, and discriminated between emitter-well and well-well transitions. We also find evidence for a resonant tunneling transition assisted by LO-phonon absorption, and a $\nu = \frac{2}{3}$ state in one of the quantum wells.

References

- [1] E.E. Mendez, L. Esaki and W.I. Wang, *Phys. Rev. B* 33 (1986) 2893.
- [2] V.J. Goldman, D.C. Tsui and J.E. Cunningham, *Phys. Rev. B* 36 (1987) 7635.
- [3] L. Eaves et al., *Appl. Phys. Lett.* 52 (1988) 212.
- [4] M.L. Leadbeater et al., *Phys. Rev. B* 39 (1989) 3438.
- [5] G.S. Boebinger, A.F.J. Levi, S. Schmitt-Rink, A. Passner, L.N. Pfeiffer and K.W. West, *Phys. Rev. Lett.* 65 (1990) 235.
- [6] M.A. Reed, W.R. Frensley, W.M. Duncan, R.J. Matyi, A.C. Seabaugh and H.-L. Tsai, *Appl. Phys. Lett.* 54 (1989) 1256.
- [7] M.L. Leadbeater, E.S. Alves, F.W. Sheard, L. Eaves, M. Henini, O.H. Hughes and G.A. Toombs, *J. Phys.: Condens. Matter* 1 (1989) 10605.
- [8] L. Eaves et al., *Solid-State Electronics* 32 (1989) 1101.
- [9] J. Leo and A.H. MacDonald, *Phys. Rev. Lett.* 64 (1990) 817.
- [10] Compare the GaAs to AlAs peak strengths in Ref. [5].
- [11] Y.O. Li, J.W. Sleight, K.J. Thomas, M.A. Reed, W.R. Frensley and Y.-C. Kao, *Bull. Am. Phys. Soc.* 37 (1992) 244.
- [12] G.S. Boebinger, A.F.J. Levi, A. Passner, L.N. Pfeiffer and K.W. West, *Phys. Rev. B* 47 (1993) 16608.